MFN= 007098
01 SID/SCD
02 5686
03 INPE-5686-PRE/1843
04 CEA
05 S
06 as
10 Batista, Paulo Prado
10 Clemesha, Barclay Robert
10 Simonich, Dale Martin
12 Seasonal variations in mesospheric sodium tidal activity
14 7435-7442
30 Journal of Geophysical Research
31 95
32 D6
40 En
41 En
42 <E>
58 DAE
61 <PI>
64 May <1990>
68 PRE
76 AERONOMIA
82 <SAO JOSE DOS CAMPOS (SP)>
83 Diurnal and nocturnal laser radar measurements of mesospheric sodium density at Sao Jose dos Campos, Brazil (23 degrees S, 46 degrees W), show strong oscillations with 12 and 24 hour periods. Data obtained in 1981 showed that atmospheric tides, mainly the vertical wind field, are the major causes of the density variations at a fixed height, thus making it possible to infer vertical wind parameters over a limited height range. In this work, 1984 and 1985 data are added to the earlier 1981 data and the 12- and 24-hour components are determined for different seasons in order to study the seasonal variations of the the tides. It is shown that the amplitudes of the oscillations in sodium density and consequently the vertical wind amplitudes, in general, are larger in winter than in ~~the~~ other seasons. Above 97 km, the semidiurnal amplitude is larger than the diurnal in winter, of the same order of magnitude at the equinoxes and smaller in summer. The phases of the inferred semidiurnal vertical wind component, above 97 km, show regular propagating characteristics with little differences between winter and equinoxes, but a confused pattern in summer. Below 93 km the wavelenghts decrease from winter to summer. In all seasons, the phase of the inferred diurnal vertical wind component stays at around 19-23 h below 85 km and above 93 km. The behavior of the phase of the diurnal oscillation in sodium density between 85 amd 90 km is quite different in the three seasons. This is explained by seasonal differences in the relative phases of the oscillations in vertical wind and density.
87 IONOSFERA
87 SODIUM

88 MIDDLE ATMOSPHERE
88 MESOSPHERIC
90 b
91 FDB-19960311
92 FDB-MLR

SEASONAL VARIATIONS IN MESOSPHERIC SODIUM TIDAL ACTIVITY

P. P. Batista, B. R. Clemesha, and D. M. Simonich

Instituto de Pesquisas Espaciais, São José dos Campos, Brazil

Abstract. Diurnal and nocturnal laser radar measurements of mesospheric sodium density at São José dos Campos, Brazil (23°S, 46°W), show strong oscillations with 12 and 24 hour periods. Data obtained in 1981 showed that atmospheric tides, mainly the vertical wind field, are the major causes of the density variations at a fixed height, thus making it possible to infer vertical wind parameters over a limited height range. In this work, 1984 and 1985 data are added to the earlier 1981 data and the 12- and 24-hour components are determined for different seasons in order to study the seasonal variations of the tides. It is shown that the amplitudes of the oscillations in sodium density and consequently the vertical wind amplitudes, in general, are larger in winter than in other seasons. Above 97 km, the semidiurnal amplitude is larger than the diurnal in winter, of the same order of magnitude at the equinoxes and smaller in summer. The phases of the inferred semidiurnal vertical wind component, above 97 km, show regular propagating characteristics with little differences between winter and equinoxes, but a confused pattern in summer. Below 93 km the wavelengths decrease from winter to summer. In all seasons, the phase of the inferred diurnal vertical wind component stays at around 19-23 h below 85 km and above 93 km. The behavior of the phase of the diurnal oscillation in sodium density between 85 and 90 km is quite different in the three seasons. This is explained by seasonal differences in the relative phases of the oscillations in vertical wind and density.

Introduction

The atmospheric region that comprises the upper mesosphere and lower thermosphere, from approximately 70 to 110 km, displays a large number of dynamical and photochemical phenomena. The understanding of these phenomena, as well as their theoretical modeling is of great importance for understanding the overall atmosphere. Unfortunately, experimental measerements are difficult in this region: it is too high to be reached by regular measurements obtained at meteorological observatories with balloons and rockets and too low to be covered by in situ satellite measurements. Therefore different methods of measurements, direct or indirect, must be used.

The horizontal wind field which can be measured by radar methods (meteor radar, partial reflection radar, etc.) is the best described at the moment, but measurements of atmospheric densities and vertical winds are infrequent and difficult. Sodium lidar, which measures the sodium concentration from 78 to 105 km, can indirectly give information about to the propagation of atmospheric waves in this region by studying the effect of the waves on the layer.

Among the dynamical manifestations which occur at the upper mesosphere and lower thermosphere region, atmospheric tides are the more prominent. These tides, generated by solar energy absorption, mainly by the ozone and water vapor in the lower atmosphere, reach large amplitudes at sodium layer heights and thus can be detected.

The behavior of atmospheric tides in the middle atmosphere is known only in a very general way (see the review by *Forbes*[1984], for example). It is important, at the moment, to know the details of the seasonal and latitudinal variations, mainly for the less known atmospheric fields, like the vertical wind and density, especially at low latitudes.

In a previous paper,*Batista et al.*[1985] analyzed sodium density data obtained in 1981, which showed strong oscillations of the layer with 12-and 24-hour periods. These oscillations were considered to be caused by the action of the vertical tidal wind in the layer. *Batista et al.*[1985] discussed the validity of assuming the sodium layer as a passive tracer of the dynamical processes at the 80-105 km region. They concluded that this approximation is good, since the chemical time constants [*Kirchhoff and Clemesha*, 1983] are large compared with tidal periods. Also the possible effects of source modulation and of the Na^+ ions have been shown to be small. The photochemical effects appeared to be important only at the very lower edge of the layer as modeled by *Kirchhoff* [1983] and experimentally investigated during evening twilight by *Kirchhoff et al.* [1986]. *Kwon et al.* [1987] also showed the presence of very strong semidiurnal oscillations in the sodium layer at a mid-latitude station (Urbana, Illinois (40°N, 88°W)).

In this work, data obtained in 1984 and 1985 were added to the 1981 data and grouped according to season in order to study the seasonal variations of the tides.

Measurements

The laser radar located at São José dos Campos, Brazil (23°12'S, 45°51'W), has been used to measure the free sodium concentration in the 78 to 105 km region since 1972. The first measurements were reported by *Kirchhoff and Clemesha* [1973]. Daytime measurements became possible after 1981, following considerable improvement of the observational technique. This made it possible to study the diurnal variation of the sodium layer [*Clemesha et al.*, 1982] and the nature of the interactions between the layer and the tides.

For the data analyzed here the sodium density was obtained with a height resolution of 1 km. The time resolution was variable, since each profile was obtained after a certain number of laser shots had been accumulated,

but generally profiles were produced at 7.5- or 15-min interval. Experimental errors in the profiles are proportional to the square root of the counting rate. Generally, the number of laser shots used to produce a profile were chosen such that an accuracy better than 10% was obtained near the layer peak for each individual profile. During daytime measurements the number of shots and the transmitted energy were increased in order to assure an accuracy similar to that of the nighttime data. Since we are interested in studying the average characteristics of variations with 12- and 24-hour periods, over a long time interval (months), hourly means of all individual profiles obtained within each one hour period were made.

The data were grouped by season (equinoxes, winter and summer) and also the general average was obtained. Data from May, June, and July were grouped as winter, November, December and January as summer, and the remaining data as equinox. In practice, it was not possible to get data during December and January, but since the amount of data obtained in November was sufficient to give a reasonable average and this average has a behavior different to that for winter and equinox, the November data were considered separately as representing summer conditions. In Table 1 we show the number of days of measurements used in the averages, classified according to months. It is observed that a considerable number of data were obtained from April to November. In Table 2 are shown the number of individual profiles used to obtain the average hourly values. As can be observed from Table 2, a minimum of 16 and a maximum of 108 individual profiles were considered for the hourly means, so that the errors in the average hourly profiles were reduced from 1/4 to 1/10 of that for the individual profiles. One can observe that a smaller number of profiles is obtained near noon and in the early morning, but only one gap occurred at 1300 LT for summer which was covered by interpolation.

TABLE 1. Number of Days With Data for Each Month

	Month											
Year	J	F	M	A	M	J	J	A	S	O	N	D
1981				4	10		6	6	2			
1984						11			6	7		
1985										5	8	

TABLE 2. Number of Profiles in the Hourly Means

	Time											
	00	01	02	03	04	05	06	07	08	09	10	11
S	30	28	31	28	27	26	30	19	18	24	28	29
W	86	89	93	76	51	52	57	45	33	68	82	76
E	50	45	41	34	37	41	43	32	26	36	50	37
	Time											
	12	13	14	15	16	17	18	19	20	21	22	23
S	17	0	16	25	26	43	43	37	40	36	35	35
W	96	89	96	100	104	102	108	92	80	79	83	87
E	47	41	42	48	64	71	83	79	59	54	61	57

Note: S(Summer), W(Winter), and E(Equinox)

Figure 1 shows contour plots of sodium density as a function of time (from 0 to 24 hours) and height (from 80 to 105 km). The contours are given in units of 10^9 .m^{-3}. Figures 1*a*-1*d* refer to equinox, summer, winter, and general average, respectively. Since the total sodium content has a very marked seasonal variation at our station [*Simonich et al.*, 1979], increasing by nearly 50% from summer to winter for this specific set of data, the general average for the sodium density showed in Figure 1*d* is somewhat biased toward winter/equinox conditions. To generate these contours, the data were smoothed by using a running average of three points in time and three points in height. Note that the general features of the variations in all seasons are the same, with a clear semidiurnal oscillation at the topside of the layer, a confused pattern near the layer peak, followed by another semidiurnal dominance below the peak and a dominant diurnal variation in the lower extremity of the layer. The more evident difference between the three seasons is the very regular and apparently dominant semidiurnal component at almost all heights during winter. It is also important to observe that the average variation does not differ significantly from the average variation given by *Batista et al.* [1985] when only data from 1981 were used.

12- and 24-Hour Components

In order to study quantitatively the 12- and 24-hour components of the oscillations shown in Figure 1, a least mean square fit method is used. At a given height h_0 the temporal variation of the sodium density is approximated by

$$Na(h_0) = A_0(h_0) + A_d(h_0)\cos\frac{2\pi}{24}[t - \phi_d(h_0)] + A_s(h_0)\cos\frac{2\pi}{12}[t - \phi_s(h_0)]$$

Where $A_0(h_0)$ is the diurnal average density at $h = h_0$, $A_d(h_0)$ and $A_s(h_0)$ are the diurnal and semidiurnal amplitudes, respectively, and $\phi_d(h_0)$ and $\phi_s(h_0)$ are the phases of the diurnal and semidiurnal components. Standard routines given by *Bevington* [1969] were used to determine these parameters. Experimental errors for each profile were used for weighting the least squares fits and the errors in amplitude, phase, and amplitude ratios were determined by using error propagation formulas.

The ratios between the amplitudes A_d/A_0 and A_s/A_0 are shown in Figures 2*a* - 2*d* for equinox, summer, winter, and general average, respectively. The more noticeable characteristics present in this figures are (1) the very large amplitudes below 83 km, (2) the dominance of the semidiurnal component above 97 km in winter, similar diurnal and semidiurnal amplitudes in equinoxes and the dominance of the diurnal in summer, and (3) near the layer peak, the amplitudes are small and the relative behavior of the components is very complicated.

The phases (ϕ_d for diurnal and ϕ_s for semidiurnal) are shown at Figures 3*a* and 3*b*, respectively. The general characteristics, namely, the height propagating phase for the semidiurnal oscillations and a phase almost fixed

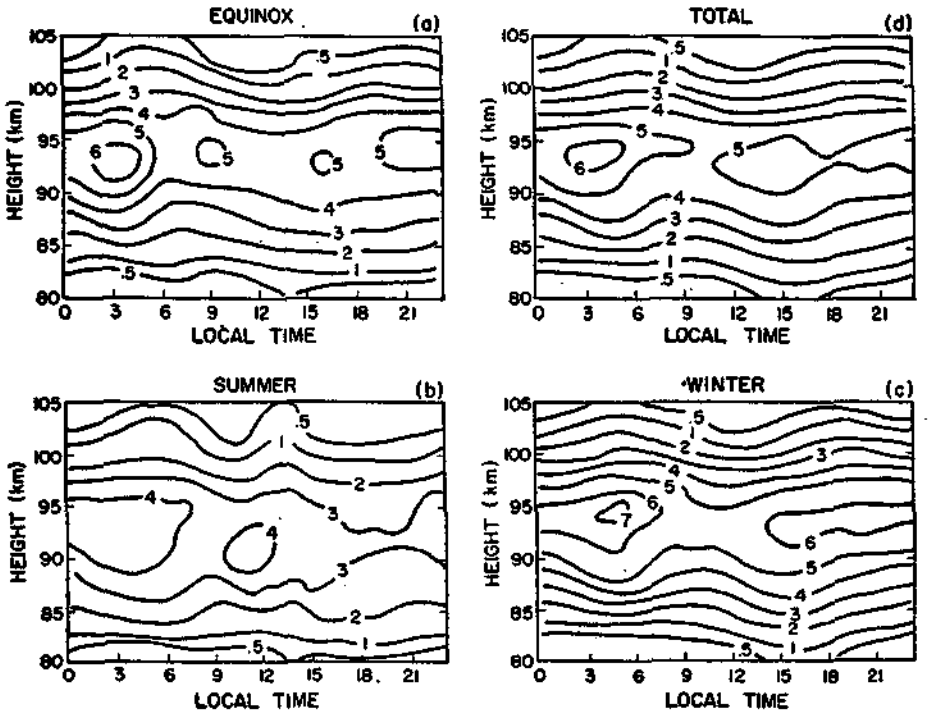

Fig. 1. Contour plots of the sodium density in units of 10^9 atoms. m^{-3} for (*a*) equinox, (*b*) summer, (*c*) winter, and (*d*) general average.

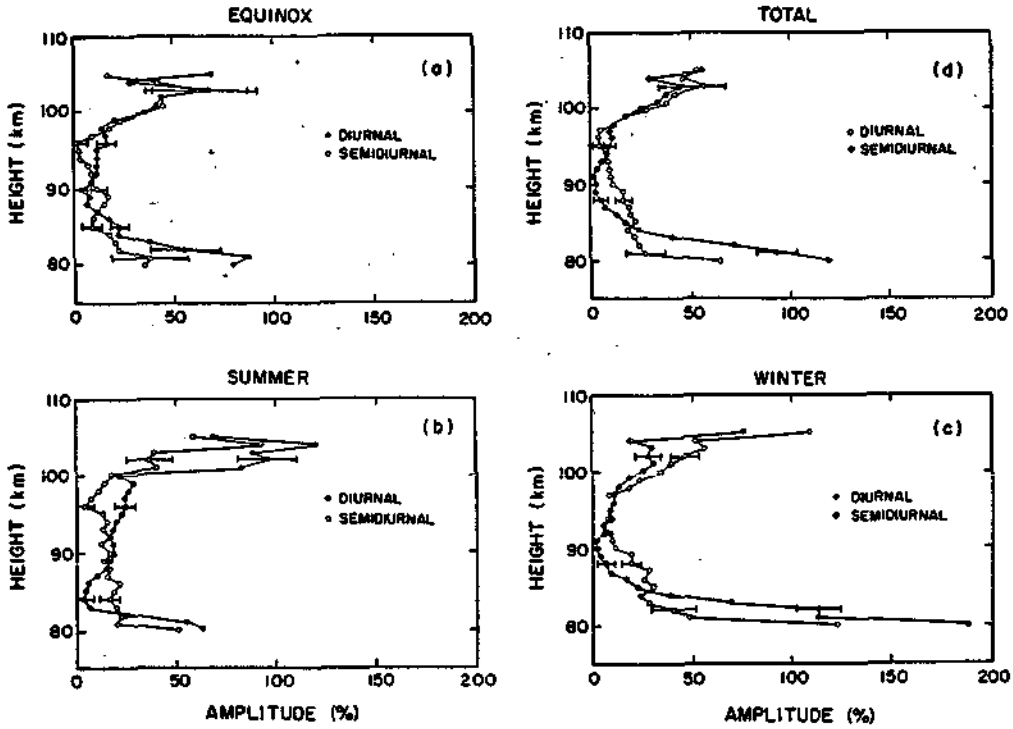

Fig. 2. Percentage ratios between the fitted diurnal amplitudes A_d/A_o (solid circles) and semidiurnal A_s/A_o (open circles) for (*a*) equinox, (*b*) summer, (*c*) winter, and (*d*) the general average. The error bars represent the standard error of the estimate.

with height for the diurnal oscillation are maintained for all seasons. For the semidiurnal case (Figure 3*a*), above ≈97 km the phase variation is very similar for winter and equinoxes but differs significantly for summer. This difference may not be very representative, since for summer the number of data is small and the relative amplitude of the semidiurnal component is small in this height range. The phase inversion occurs between 93 and 96 km for all seasons. Below 93 km, there is a strong seasonal variation of the vertical wavelength, with smaller wavelengths occurring in summer, increasing towards the equinoxes, and maximizing in winter.

Concerning the diurnal component (Figure 3*b*), the phase stays at around 1600 LT below 85 km for equinoxes and winter but is very scattered for summer. The phase change is less abrupt than in the semidiurnal case , occurring from 85 to 91 km. Above 91 km, for summer, the phase remains at around 0400 LT, but increases with height for equinoxes and winter.

Discussion

According to the reasoning followed in a previous paper [*Batista et al.*, 1985], the effect of tides in the mesospheric sodium layer can be expressed at first approximation by

$$\frac{\Delta n}{n_0} = \frac{\Delta N}{N_0} + \frac{iT}{2\pi}\left(\frac{1}{n_0}\frac{dn_0}{dh} - \frac{1}{N_0}\frac{dN_0}{dh}\right)W \qquad (1)$$

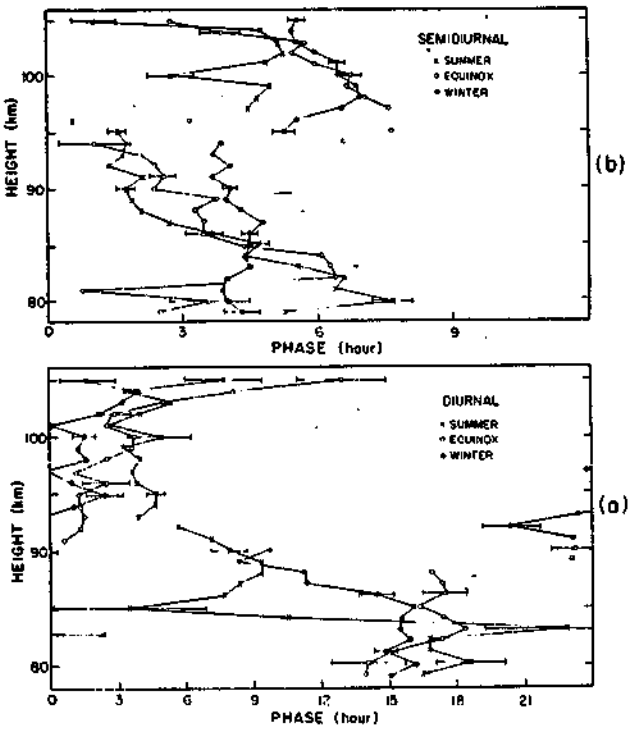

Fig. 3. Phase of the (*a*) diurnal and (*b*) semidiurnal (b) fitted amplitudes expressed as the hour of maximum occurrence of sodium density. Solid circles for winter, open circles for equinox, and crosses for summer.

Where n and N refer to sodium and atmospheric densities, respectively. Subscript zero refers to the unperturbed state, Δ to the perturbation; T is the period of the oscillation, h is the height, and W is the vertical wind amplitude. The analysis of formula (1) leads us to conclude that at the lower and upper extremities of the layer the effect of the vertical wind (second term in (1)) is dominant over the first term. This makes $\Delta n/n_0$ follow the phase of W, leading 90° on the topside and lagging 90° on the bottomside. This 180° phase jump is observed in both the semidiurnal and diurnal cases in Figure 3. Also the general features of Figure 2 are explained by (1). Near the layer peak the fractional variation of n is of the same order as that of the atmospheric density fluctuation, but it increases substantially towards the borders. It is interesting to notice that the first term of the right-hand side of (1), although not very important far from the peak, it is important in determining the height and how fast the phase transition occurs. Not only the amplitude of $\Delta N/N_o$ but also the relative importance of $\Delta N/N_o$ and W can substantially alter the behavior of $\Delta n/n_o$ near the peak. To show this fact, we have made a simulation using (1) with a simple tidal model which approximately reproduces the observed diurnal and semidiurnal oscillations, and a model n_o which is the average sodium density at our station. A constant value of $\Delta N/N_o$=0.07 both for diurnal and semidiurnal cases and W=4 cm. s^{-1} and 10 cm. s^{-1} for the diurnal and semidiurnal cases, respectively, were used. The results are shown in Figures 4*a* and 4*b* for the diurnal and semidiurnal simulation, respectively. We have varied only the relative phase difference ($\Delta\phi$) between W and ΔN. In the figure, ΔN represents the assumed phase for the atmospheric density perturbation, $W1$, $W2$, and $W3$ the assumed phases for W, and $T2$ is the total effect of the second term of the right-hand side of (1). One can see that in all cases the phase of Δn tends to follow $T2$ far from the peak, but the transition near the peak can occur in a very complicated way, depending on the phase difference between $\Delta N/N_o$ and W. Also the relative importance of $\Delta N/N_o$ and W and the shape of the average profile n_o can affect this phase variation near the peak.

The estimated phases are compared with the results of tidal models by *Forbes* [1982*a*,*b*], which include the seasonal variation. The phases of the vertical wind (hour of maximum) at 24° latitude for equinox, winter and summer, taken from a complete tabulation of the tidal fields [*Forbes and Gillette*, 1982] are shown in Figure 5. Also shown are the phases of $\Delta n/n_0$, displaced −90° above and +90° below the peak, which should be compared with W according to the previous discussion. For the semidiurnal component there is a good agreement between the model and the inferred vertical wavelength for the equinoxes (Figure 5*a*), but there is a consistent phase shift with the theoretical phase leading the experimental one by about 1 hour. For the winter, there is a large phase difference between the model and the data, with the model leading the inferred phase by 3-4 hours. Despite this big difference in the relative phase, it is interesting to note that only for winter do both the model and

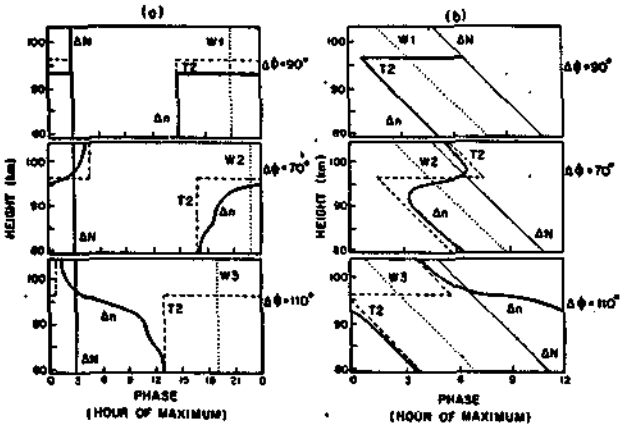

Fig. 4. Simulated phase of Δn (thick solid lines) obtained from (1) by varying the phase differences between ΔN (thin solid lines) and W (dotted lines), in wave models which approximate the (*a*) diurnal oscillation and (*b*) semidiurnal. T2 (dashed lines) represents the second term in (1).

the data show the change from a pure downward phase propagation above 90 km to a situation of a constant variation with height or even a decreasing phase with decreasing height, below this height. For the summer, it appears that there is a tendency for smaller wavelengths be dominant at low altitudes. This characteristic is apparent in both the model and the data (Figure 5*c*), although there is also the systematic phase shift with the model leading the data by $\approx$2 hours. It is important to notice that from 90 to 105 km the experimental phases do not vary appreciably with season, while for the model there is a 2-hour difference between winter and equinox.

For the diurnal component the lack of vertical downward phase propagation observed in the 1981 data analysis [*Batista et al.*, 1985] is observed for all seasons. The phase variation with height above 90 km hardly exists for summer (Figure 5*f*) and has a small upward propagation for winter and equinox. Below the layer peak there is some evidence for phase propagation in summer and winter but not for equinox. The Forbes' model predicts

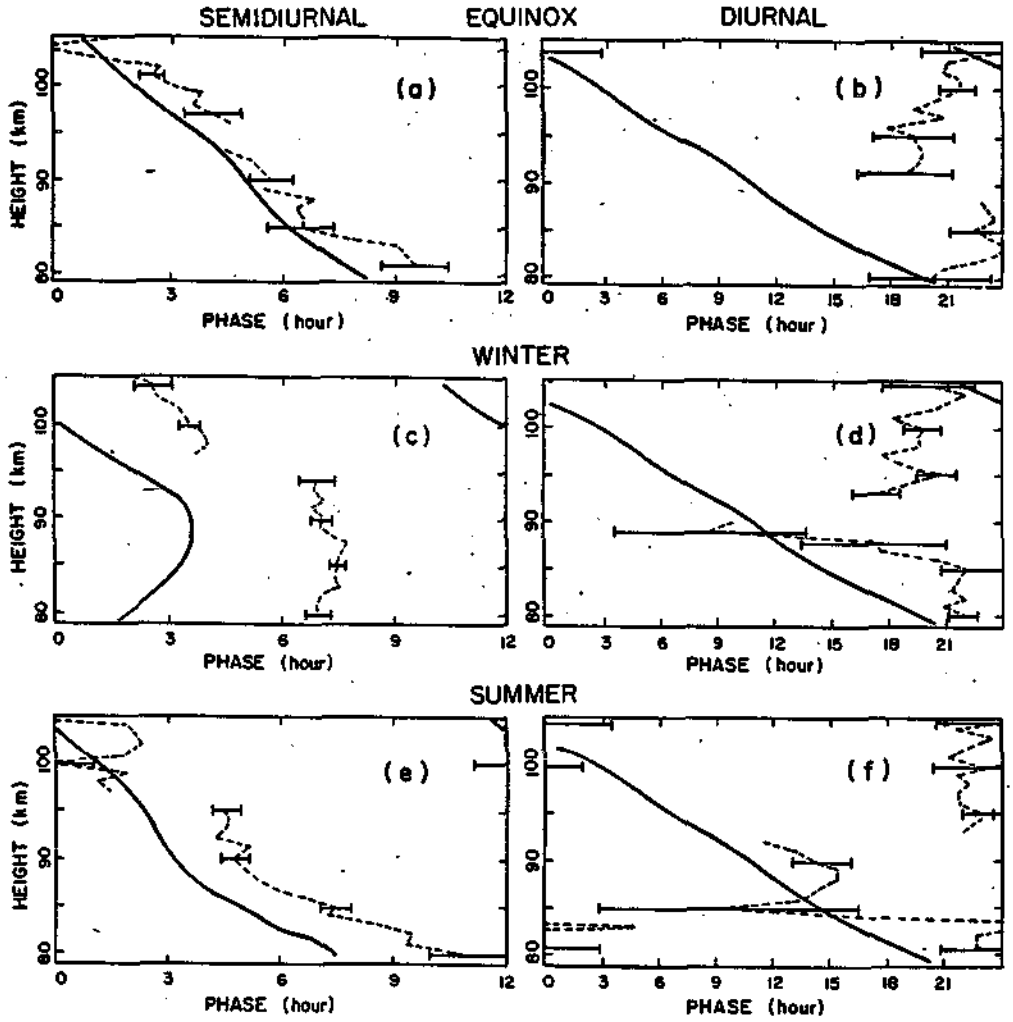

Fig. 5. Comparison between the phase of vertical wind at 24° S from Forbes' model and the inferred phase using lidar data. (*a*, *c*, and *e*) represent the semidiurnal phases for equinox, winter, and summer, respectively, and (*b*, *d*, and *f*) the corresponding phases for the diurnal case. Solid lines refer to theory, and dashed lines to the observations.

a downward phase propagation with small seasonal variation and a vertical wavelength of ≈25-30 km.

Measurements of tidal fields at low latitude are very scarce. Most of the available data refer to the east-west or north-south winds obtained in specific measurement campaigns usually covering an interval of only a few days. These measurements have generally shown a dominant $S_{1,1}$ propagating mode with amplitude greater than the semidiurnal and a tendency for the oscillation to break at ≈90 km. *Mathews* [1976], at Arecibo (18°N) observed, a dominant $S_{1,1}$ mode in 2 days of measurements of the eastward and southward wind from 85 to 100 km. Similar results were obtained by *Bernard et al.* [1981], who observed the zonal wind at Punta Borinquen, Puerto Rico (18°N), for periods of nearly 7 days for each season and concluded that as a rule the diurnal tide was strong and stable, consistent with the $S_{1,1}$ mode. Yet, *Vincent and Ball* [1981] measured the east-west and north-south wind in November and June from 80 to 98 km at Townsville, Australia (19°S), and observed that for November (summer) the diurnal oscillation was strong and regular, consistent with the $S_{1,1}$ mode dominance, but for June (winter) the diurnal oscillation was weakened and dominated by evanescent modes. *Kent et al.* [1972] measured the atmospheric density fluctuations with a lidar from 68- to 100-km altitude at Kingston, Jamaica (18°N), and observed oscillations with inferred period of 24 hours and vertical wavelength consistent with the $S_{1,1}$ and $S_{1,3}$ tidal mode. The analysis of a more complete set of data [*Kent and Keenliside*, 1975] showed that the $S_{1,3}$ was indeed a dominant feature in the density field in that height range and latitude.

Care must be taken in comparing our data with the previous low-latitude observations, because they refer to different atmospheric fields and latitudes. Although related to each other, the latitudinal structures of the various tidal fields are different. For the vertical wind and density the latitudinal expansions are the Hough functions, while for the east-west and north-south wind there are different latitudinal expansions [*Chapman and Lindzen*, 1970]. *Kent and Keenliside* [1975] explained the dominance of the $S_{1,3}$ mode at the density field in 18°N (different from the dominance of $S_{1,1}$ in the horizontal winds) on the basis in the existence of a null of the $S_{1,1}$ latitudinal expansion in 18°N for the density but a dominance of this mode for the horizontal winds. For our latitude 23°S, there is not a null of $S_{1,1}$, but it is expected that many propagating modes should contribute with similar amplitudes, and that the evanescent modes should also contribute substantially. It is not at all surprising that for an average of various days of measurements, the propagating modes, which are very sensitive to variations of the source and the conditions of propagation from the lower to the upper atmosphere, tend to interfere destructively permitting that evanescent modes stand out.

More recent tidal models [*Vial*, 1986; *Forbes and Hagan*, 1988] have given emphasis to the propagation characteristics of the diurnal tide. It is shown that the presence of mean winds and dissipation can have a strong effect on the propagation characteristics of the $S_{1,1}$ diurnal mode, producing significant asymmetries about the equator during solstice and increasing the vertical wavelength with height from 80 to 100 km. They also showed that the null point for the $S_{1,1}$ tide can be shifted in latitude owing to the effect of mean winds. Since our station is located near this null point, small variations in the mean winds would result in large differences in the relative mode domination in the diurnal tide.

Conclusions

The analysis of a larger number of data has confirmed the existence of consistent oscillations with periods of 12 and 24 hours in the mesospheric sodium layer. Owing to the linear interaction between the tidal wave and the layer, it has been possible to infer the phases of the vertical winds responsible for the variation and the relative importance of the diurnal and semidiurnal amplitudes. Separating these data for equinox, winter, and summer, one can see substantial differences in the amplitudes and phases with season. Generally, the amplitudes are larger in winter, a behavior which is not predicted by the *Forbes'* [1982*a*,*b*] model. For the semidiurnal tide, the agreement between the theoretical results and the data is satisfactory with respect to the vertical wavelengths, but a consistent phase difference is apparent. The transition from very long wavelength below to smaller wavelength above 90 km, as predicted by theory is shown by the data.

The difference between the diurnal tide predicted by theory and the present data is remarkable. Part of the variation of the sodium density, mainly at the very bottom of the layer, may be due to photochemical effects [*Kirchhoff*, 1983], and it would be interesting in a further step to include this effect in the tidal analysis. Above this height, the photochemical effect shoud be small, probably negligible as compared with the tidal amplitudes.

Acknowledgments. We are grateful to our colleagues V. W. J. H. Kirchhoff and Hisao Takahashi for data collection and helpful discussions. This work was partially supported by the Fundo Nacional de Desenvolvimento Científico e Tecnológico (FNDCT) under contract FINEP-537/CT.

References

Batista, P. P., B. R. Clemesha, D. M. Simonich, and V. W. J. H. Kirchhoff, Tidal oscillations in the atmospheric sodium layer, *J. Geophys. Res.*, *90*, 3881-3888, 1985.

Bernard, R., J. L. Fellous, M. Massebeuf, and M. Glass, Simultaneous meteor radar observations at Mompazier (France, 44° N) and Punta Borinquen (Puerto Rico, 18° N), I, Latitudinal variations of atmospheric tides, *J. Atmos. Terr. Phys.*, *43*, 525-533, 1981.

Bevington, P. R., *Data Reduction and Error Analysis for the Physical Sciences*, McGraw-Hill, New York, 1969.

Chapman S. and R. S. Lindzen, *Atmospheric Tides*, D. Reidel Publ. Co., Ma. U.S.A., 1970.

Clemesha, B. R., D. M. Simonich, P. P. Batista and V. W. J. H. Kirchhoff, The diurnal variation of atmospheric sodium, *J. Geophys. Res.*, *87*, 181-186, 1982.

Forbes, J. M., Atmospheric tides, 1, Model description and results for the solar diurnal component, *J. Geophys. Res.*, *87*, 5222-5240, 1982*a*.

Forbes, J. M., Atmospheric tides, 2, The solar and lunar semidiurnal components, *J. Geophys. Res.*, *87*, 5241-5252, 1982*b*.

Forbes, J. M., Middle atmosphere tides, *J. Atmos. Terr. Phys.*, *46*, 1049-1067, 1984.

Forbes, J. M. and D. F. Gillette, A compendium of theoretical atmospheric tidal structures. Part I: Model description and explicit structures due to realistic thermal and gravitational excitation, *Rep. AFGL-TR-62-0173(i)*, 193 pp., Aeronomy Div., Air Force Geophys. Lab., Hanscon Air Force Base, Mass., June 1982.

Forbes, J. M., and M. E. Hagan, Diurnal propagating tide in the presence of mean winds and dissipation: A numerical investigation, *Planet. Space Sci.*, *36*, 579-590, 1988.

Kent, G. S., and W. Keenliside, Laser radar observations of the $\Theta_3^{w,1}$ diurnal atmospheric tidal mode above Kingston, Jamaica, *J. Atmos. Sci.*, *32*, 1663-1666, 1975.

Kent, G. S., W. Keenliside, M. C. W. Sandford, and R. W. H. Wright, Laser radar observations of atmospheric tides in the 70-100 km height region, *J. Atmos. Terr. Phys.*, *34*, 373- 386, 1972.

Kirchhoff, V. W. J. H., Atmospheric sodium chemistry and diurnal variations: An up-date, *Geophys. Res. Lett.*, *10*, 721-724, 1983.

Kirchhoff, V. W. J. H., and B. R. Clemesha, Atmospheric sodium measurements at 23° S, *J. Atmos. Terr. Phys.*, *35*, 1493-1498, 1973.

Kirchhoff, V. W. J. H., and B. R. Clemesha, The atmospheric neutral sodium layer, 2, Diurnal variations, *J. Geophys. Res.*, *88*, 442-450, 1983.

Kirchhoff, V. W. J. H., P. P. Batista, B. R. Clemesha, and D. M. Simonich, The twilight sodium layer, *J. Geophys. Res.*, *91*, 13,303-13,307, 1986.

Kwon, K. H., C. S. Gardner, D. C. Senft, F. L. Roesler, and J. Harlander, Daytime lidar measurements of tidal winds in the mesospheric sodium layer at Urbana, Illinois, *J. Geophys. Res.*, *92*, 8781-8786, 1987.

Mathews, J. D., Measurements of the diurnal tides in the 80- to 100-km altitude range at Arecibo, *J. Geophys. Res.*, *81*, 4671-4677, 1976.

Simonich, D. M., B. R. Clemesha, and V. W. J. H. Kirchhoff, The mesospheric sodium layer at 23° S: Nocturnal and seasonal variations, *J. Geophys. Res.*, *84*, 1543-1550, 1979.

Vial, F., Numerical simulations of atmospheric tides for solstice conditions, *J. Geophys. Res.*, *91*, 8955-8969, 1986.

Vincent, R. A, and S. M. Ball, Mesospheric winds at low- and mid-latitudes in the southern hemisphere, *J. Geophys. Res.*, *86*, 9159-9196, 1981.

P. P. Batista, B. R. Clemesha, and D. M. Simonich, Instituto de Pesquisas espaciais, INPE, C. P. 515, 12201, São José dos Campos, SP, Brazil.